Inorg. Chem. **1987**, *26*, 3409–3413

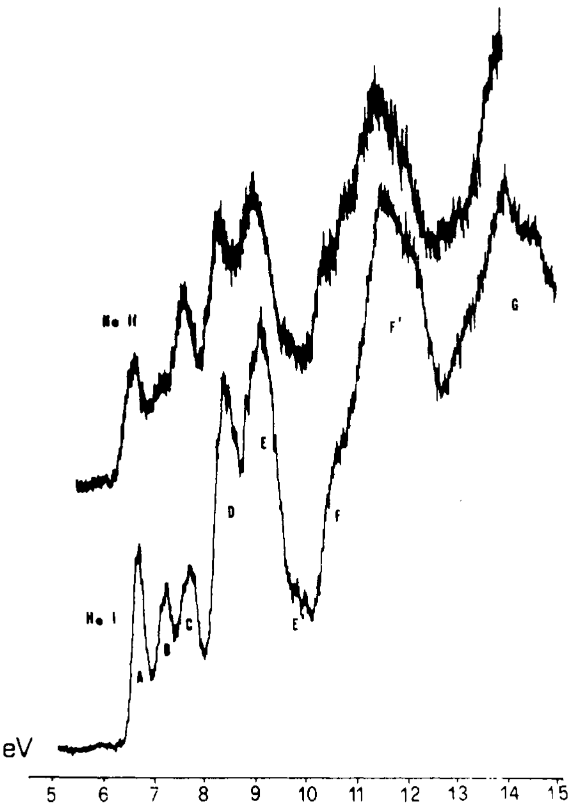

Figure 4. He I/He II excited PE spectra of $Rh_2[HC(NR)_2]_2[O_2CCF_3]_2$ (R = *p*-tolyl).

intensity variations on passing from the He I to the He II ionizing source,[15] the observed behavior can be interpreted either as a major involvement of the d metal AOs with the orbital giving rise to band A or as an indication of some component of band B arising from a ligand-localized MO. The latter hypothesis is well in tune with the theoretical results, which predict, at ca. 1.5 eV higher IE than the ionization from the HOMO, two quasi-degenerate ionizations from the $5e_g$ (π^* Rh–Rh, 95% localized on metals) and $1a_{1u}$ (100% nitrogen-based π ligand) MOs (see Table I). The presence of two components under band B is also in agreement with the splitting observed in the corresponding band of the PE spectrum of the less symmetrical complex **2** (Figure 4). The low-intensity band C (which has been confirmed by running several expanded-scale He I spectra) can be tentatively assigned to the ionization of the δ (Rh–Rh) $2b_{2g}$ MO. Its low intensity agrees well with that observed for the same ionization in the spectrum of $Rh_2(mhp)_4$.[5]

The assignments of the inner bands are complicated by the superposition of the *p*-tolyl group ionizations. We can just propose the following plausible assignments on the basis of the results of the theoretical calculations. The computed energy separations between the $4e_g$ (ligand σ/π nonbonding MO), $6e_u$ (π Rh–Rh), and $5a_{1g}$ (σ Rh–Rh) MOs lead us to ascribe their ionizations respectively to shoulder D, band E, and shoulder E′.

The He I PE spectrum of the mixed complex **2** (Figure 4) is noticeably different from that just discussed: all the bands are shifted by about 1 eV toward higher IEs, as already anticipated by our theoretical results (see Figure 2 and TSIEs in Table II). Moreover, band B of the spectrum of **3** is now split into two well-resolved components (B + C) and band D, a shoulder of band E in the previous case, is now a resolved band with an intensity comparable to that of band E. In this regard we must remember that in **2** we have only half of the aromatic rings (whose ionizations contribute to band E) that were present in the tetraformamidinate complex **3**. Very important experimental evidence is related to the change of the relative intensity between bands B and C on passing to the He II spectrum (Figure 4): the large falloff of intensity of band B is diagnostic of localization on the ligand of the corresponding MO.[15]

As in the previous case, band A is safely assigned to ionization from the $10b_1$ (δ^*) HOMO on the basis of the calculations. The assignment of bands B and C, however, needs some discussion. We have already pointed out that the symmetry reduction on passing from **3** to **2** does not produce significant energy separation on the π type metal–metal orbitals (see Figure 2 and TSIEs in Table II). According to the TSIE values obtained for the model **2a**, we should assign band B to the π^* (Rh–Rh) ($9a_2$,$9b_1$) MOs (over 90% localization on the metals) and band C to the ligand-based $8a_2$ MO (over 95% on the formamidinate ligand). This assignment, however, is in contrast with two experimentl observations: (i) band B is less intense than band C in the He I spectrum; (ii) the already mentioned decrease of the relative intensity of B vs. that of C on passing to the He II spectrum. Both these points give support to the opposite assignment, i.e. band B to $8a_2$ and band C to $9a_2$ and $9b_1$ MOs. This failure of the theoretical prediction could be ascribed to the neglect of the CF_3 groups in the model adopted for the calculations.[17]

We take band D to represent the ionizations of four MOs, namely $13a_1$ (δ bonding Rh–Rh), $12a_1$ and $12b_2$ (π bonding Rh–Rh), and $8b_1$ (localized to an equal extent on both formamidinate and carboxylate ligands). Finally, in analogy with the assignment of **3**, we propose the assignment of the $11a_1$ (σ bonding Rh–Rh) MO to the weak shoulder E′.

In conclusion, we want to stress here that the present analysis of the UV-PE data on Rh_2^{4+} formamidinate complexes furnishes an electronic configuration ($\sigma^2\pi^4\delta^2\pi^{*4}\delta^{*2}$) identical with that obtained by a previous UV-PE study on the quite different $Rh_2(mhp)_4$ complex.[5] On the other hand, all the available Xα type theoretical results[4a] (the most rigorous treatment for such complicated molecules to date) are in agreement in predicting similar configurations in both carboxylate and formamidinate complexes. We could suggest, then, that this bonding scheme can be considered as peculiar to the Rh_2^{4+} arrangement.

Acknowledgment. Financial support for this study from the Ministero della Pubblica Istruzione (Rome) is gratefully acknowledged.

Registry No. 2, 109976-30-9; 3, 108149-48-0.

---

(15) In fact, on the basis of the Gelius model for the molecular photoionization cross sections,[16] we expect a marked decrease in relative intensity for those bands containing ligand-localized ionizations with respect to metal *n*d-based ones on passing from the He I to the He II excitation source.

(16) Gelius, U. In *Electron Spectroscopy*; Shirley, D. A., Ed.; North-Holland: Amsterdam, 1972; p 311.

(17) Actually, when one deals with a less symmetrical molecule, such as **2**, the errors induced by adopting a simplified model may not be balanced. In this case, the $9a_2$ and $9b_1$ MOs have a larger localization on the carboxylate ligands than the $8a_2$ MO, so that the neglect of the large electron-withdrawing effect of the CF_3 substituents produces a shift toward lower IEs of the $9a_2$ and $9b_1$ MOs.

Contribution from the Department of Chemistry
and Biochemistry, University of California,
Los Angeles, California 90024-1569

Synthesis and Molecular Structures of *closo*-3-(η^6-$CH_3C_6H_5$)-3,1,2-$FeC_2B_9H_{11}$ and *closo*-3-(η^6-1,4-$(CH_3)_2C_6H_4$)-3,1,2-$FeC_2B_9H_{11}$

Han Chyul Kang, Carolyn B. Knobler,
and M. Frederick Hawthorne*

Received April 16, 1987

The chemistry of mixed-sandwich transition-metal complexes of the type [(η^6-arene)M(η^5-Cp)] has been well documented in literature.[1] In view of the close structural and electronic similarity

0020-1669/87/1326-3409$01.50/0

Table I. Selected Bond Distances and Angles for **1**

	Bond Distances (Å)		
Fe(03)–C(01)	2.043 (13)	Fe(03)–C(02)	2.049 (13)
Fe(03)–B(04)	2.082 (15)	Fe(03)–B(07)	2.065 (15)
Fe(03)–B(08)	2.140 (14)	Fe(03)–C(31)	2.09 (2)
Fe(03)–C(32)	2.082 (16)	Fe(03)–C(33)	2.090 (10)
Fe(03)–C(34)	2.11 (2)	Fe(03)–C(35)	2.11 (2)
Fe(03)–C(36)	2.105 (11)	C(01)–C(02)	1.60 (2)
C(01)–B(04)	1.67 (2)	C(01)–B(05)	1.70 (2)
C(01)–B(06)	1.72 (2)	C(02)–B(06)	1.73 (2)
C(02)–B(07)	1.69 (2)	C(02)–B(11)	1.67 (2)
B(04)–B(05)	1.78 (2)	B(04)–B(08)	1.76 (2)
B(04)–B(09)	1.82 (2)	B(07)–B(08)	1.75 (2)
B(07)–B(11)	1.80 (2)	B(07)–B(12)	1.80 (2)
B(08)–B(09)	1.78 (2)	B(08)–B(12)	1.81 (2)
	Bond Angles (deg)		
C(01)–Fe(03)–C(02)	46.1 (5)	C(01)–Fe(03)–B(04)	47.8 (6)
C(01)–Fe(03)–B(07)	81.9 (6)	C(01)–Fe(03)–B(08)	82.3 (5)
C(01)–Fe(03)–C(35)	97.9 (6)	C(01)–Fe(03)–C(36)	103.6 (6)
C(02)–Fe(03)–B(04)	82.0 (6)	C(02)–Fe(03)–B(07)	48.6 (5)
C(02)–Fe(03)–B(08)	82.9 (5)	C(02)–Fe(03)–C(31)	100.1 (6)
C(02)–Fe(03)–C(36)	100.0 (6)	B(04)–Fe(03)–B(08)	49.3 (6)
B(04)–Fe(03)–C(34)	92.9 (6)	B(04)–Fe(03)–C(35)	104.5 (6)
B(07)–Fe(03)–B(08)	49.3 (5)	B(07)–Fe(03)–C(31)	100.5 (6)
B(07)–Fe(03)–C(32)	94.4 (6)	B(08)–Fe(03)–C(32)	103.5 (6)
B(08)–Fe(03)–C(33)	92.2 (6)	C(31)–Fe(03)–C(32)	39.1 (6)
C(31)–Fe(03)–C(36)	38.9 (6)	C(32)–Fe(03)–C(33)	39.1 (6)
C(33)–Fe(03)–C(34)	38.8 (6)	C(34)–Fe(03)–C(35)	38.6 (6)
C(35)–Fe(03)–C(36)	38.6 (6)	C(02)–C(01)–B(04)	111.7 (10)
C(01)–C(02)–B(07)	109.6 (10)	C(01)–B(04)–B(08)	106.4 (10)
C(02)–B(07)–B(08)	107.1 (10)	B(04)–B(08)–B(07)	105.0 (10)

of the dicarbollide ligand to that of the cyclopentadienyl ligand,[2] the former would be expected to form analogous mixed-ligand complexes with arenes and transition metals. However, although other carborane complexes have been reported,[3] only a few dicarbollide complexes appear in the literature.[3a,b,f] As part of our ongoing investigation of metallacarborane derivatives, we have prepared (η^6-arene)ferracarborane complexes incorporating toluene (*closo*-3-(η^6-$CH_3C_6H_5$)-3,1,2-$FeC_2B_9H_{11}$(**1**)) or *p*-xylene (*closo*-3-(η^6-1,4-$(CH_3)_2C_6H_4$)-3,1,2-$FeC_2B_9H_{11}$(**2**)) directly from the reactions of K[*nido*-7,8-$C_2B_9H_{12}$], ferric chloride, and triethylamine in either toluene or *p*-xylene solution. This simple route for the formation of (η^6-arene)ferracarborane, was originally employed for the synthesis of boron-substituted carborane cage derivatives by using ferric chloride promoted oxidative coupling of K[*nido*-7,8-$C_2B_9H_{12}$] with Lewis base L.[4]

$$\mathrm{K}[nido\text{-}7,8\text{-}C_2B_9H_{12}] + 2FeCl_3 + L \rightarrow nido\text{-}7,8\text{-}C_2B_9H_{11}L + 2FeCl_2 + HCl + KCl$$

Both symmetrically and asymmetrically substituted zwitterionic neutral carboranes[5] *nido*-10-$N(C_2H_5)_3$-7,8-$C_2B_9H_{11}$[6] and *nido*-9-$N(C_2H_5)_3$-7,8-$C_2B_9H_{11}$[7] were found in the above reaction mixture and characterized by spectroscopic techniques. While

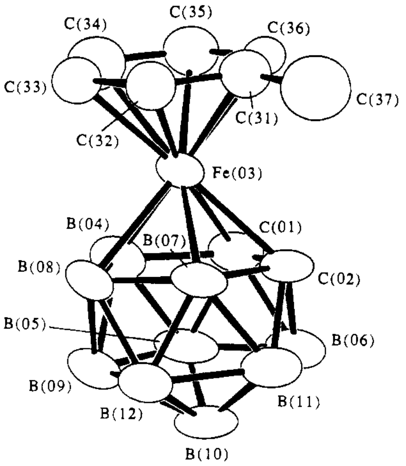

Figure 1. Molecular structure *closo*-3-(η^6-$CH_3C_6H_5$)-3,1,2-$FeC_2B_9H_{11}$ (**1**) showing the atom-labeling scheme. All hydrogen atoms have been omitted for clarity.

Table II. Selected Bond Distances and Angles for **2**

	Bond Distances (Å)		
Fe(03)–C(01)	2.040 (10)	Fe(03)–C(02)	2.044 (11)
Fe(03)–B(04)	2.116 (11)	Fe(03)–B(07)	2.104 (13)
Fe(03)–B(08)	2.110 (11)	Fe(03)–C(31)	2.130 (9)
Fe(03)–C(32)	2.095 (9)	Fe(03)–C(33)	2.094 (9)
Fe(03)–C(34)	2.132 (9)	Fe(03)–C(35)	2.113 (9)
Fe(03)–C(36)	2.127 (9)	C(01)–C(02)	1.633 (13)
C(01)–B(04)	1.706 (14)	C(01)–B(05)	1.721 (16)
C(01)–B(06)	1.742 (16)	C(02)–B(06)	1.719 (15)
C(02)–B(07)	1.706 (15)	C(02)–B(11)	1.700 (15)
B(04)–B(05)	1.797 (15)	B(04)–B(08)	1.772 (15)
B(04)–B(09)	1.752 (15)	B(05)–B(06)	1.745 (17)
B(05)–B(09)	1.736 (15)	B(05)–B(10)	1.736 (16)
B(06)–B(10)	1.764 (15)	B(06)–B(11)	1.783 (16)
B(07)–B(08)	1.797 (17)	B(07)–B(11)	1.788 (17)
B(07)–B(12)	1.760 (17)	B(08)–B(09)	1.806 (15)
B(08)–B(12)	1.808 (15)	B(09)–B(10)	1.746 (15)
B(09)–B(12)	1.777 (15)	B(10)–B(11)	1.791 (16)
B(10)–B(12)	1.811 (15)	B(11)–B(12)	1.757 (15)
C(31)–C(32)	1.404 (13)	C(31)–C(36)	1.416 (14)
C(31)–C(37)	1.523 (17)	C(32)–C(33)	1.417 (14)
C(33)–C(34)	1.430 (16)	C(34)–C(35)	1.379 (13)
C(34)–C(38)	1.515 (15)	C(35)–C(36)	1.427 (14)
	Bond Angles (deg)		
C(01)–Fe(03)–C(02)	47.14 (38)	C(01)–Fe(03)–B(04)	48.40 (41)
C(01)–Fe(03)–B(07)	83.90 (46)	C(01)–Fe(03)–B(08)	83.76 (40)
C(01)–Fe(03)–C(35)	100.39 (36)	C(01)–Fe(03)–C(36)	98.31 (38)
C(02)–Fe(03)–B(04)	82.56 (44)	C(02)–Fe(03)–B(07)	48.53 (41)
C(02)–Fe(03)–B(08)	83.39 (42)	C(02)–Fe(03)–C(31)	96.80 (41)
C(02–Fe(03)–C(36)	103.99 (40)	B(04)–Fe(03)–B(08)	49.59 (40)
B(04)–Fe(03)–C(34)	94.76 (43)	B(04)–Fe(03)–C(35)	98.95 (43)
B(07)–Fe(03)–B(08)	50.48 (46)	B(07)–Fe(03)–C(31)	104.93 (45)
B(07)–Fe(03)–C(32)	91.19 (45)	B(08)–Fe(03)–C(33)	91.53 (42)
B(08)–Fe(03)–C(34)	101.95 (41)	C(31)–Fe(03)–C(32)	38.80 (35)
C(31)–Fe(03)–C(36)	38.85 (37)	C(32)–Fe(03)–C(33)	39.54 (39)
C(33)–Fe(03)–C(34)	39.53 (42)	C(34)–Fe(03)–C(35)	37.91 (35)
C(35)–Fe(03)–C(36)	39.34 (40)	C(02)–C(01)–B(04)	110.60 (82)
C(01)–C(02)–B(07)	112.13 (87)	C(01)–B(04)–B(08)	105.63 (77)
C(02)–B(07)–B(08)	104.18 (86)	B(04)–B(08)–B(07)	107.42 (77)
Fe(03)–C(31)–C(37)	130.55 (87)	C(32)–C(31)–C(36)	120.00 (88)
C(32)–C(31)–C(37)	120.16 (89)	C(36)–C(31)–C(37)	119.74 (84)
C(31)–C(32)–C(33)	120.25 (92)	C(32)–C(33)–C(34)	119.79 (88)
Fe(03)–C(34)–C(38)	131.29 (72)	C(33)–C(34)–C(35	119.37 (96)
C(33)–C(34)–C(38)	119.02 (94)	C(35)–C(34)–C(38)	121.55 (108)
C(34)–C(35)–C(36)	121.49 (92)	C(31)–C(36)–C(35)	119.02 (83)

---

(1) (a) Silverthorn, W. E. *Adv. Organomet. Chem.* **1975**, *13*, 47. (b) Watts, W. E. In *Comprehensive Organometallic Chemistry*; Wilkinson, G., Stone, F. G. A., Abel, E., Eds.; Pergamon: Oxford, England, 1982; Vol. 8, Chapter 59; pp 1013–1071.

(2) (a) Hawthorne, M. F.; Young, D. C.; Wegner, P. A. *J. Am. Chem. Soc.* **1965**, *87*, 1818. (b) Hawthorne, M. F.; Young, D. C.; Andrews, T. D.; Howe, D. V.; Pilling, R. L.; Pitts, A. D.; Reintjes, M.; Warren, L. F., Jr.; Wegnere, P. A. *J Am. Chem. Soc.* **1968**, *90*, 879. (c) Hawthorne, M. F. *Acc. Chem. Res.* **1968**, *1*, 281.

(3) (a) Hanusa, T. P.; Huffman, J. C.; Todd, L. J. *Polyhedron* **1982**, *1*, 77. (b) Garcia, M. P.; Green, M.; Stone, F. G. A.; Somerville, R. G.; Welch, A. J. *J. Chem. Soc., Chem. Commun.* **1981**, 871. (c) Maynard, R. B.; Swisher, R. G.; Grimes, R. N. *Organometallics* **1983**, *2*, 500. (d) Swisher, R. G.; Sinn, E.; Grimes, R. N. *Organometallics* **1983**, *2*, 506. (e) Micciche, R. D.; Sneddon, L. G. *Organometallics* **1983**, *2*, 674. (f) Hanusa, T. P.; Huffman, J. C.; Curtis, T. L.; Todd, L. J. *Inorg. Chem.* **1985**, *24*, 787. (g) Swisher, R. G.; Sinn, E.; Butcher, R. J.; Grimes, R. N. *Organometallics* **1985**, *4*, 882. (h) Swisher, R. G.; Sinn, E.; Grimes, R. N. *Organometallics* **1985**, *4*, 890. (i) Swisher, R. G.; Sinn, E.; Grimes, R. N. *Organometallics* **1985**, *4*, 896. (j) Spencer, J. T.; Grimes, R. N. *Organometallics* **1987**, *6*, 323. (k) Spencer, J. T.; Grimes, R. N. *Organometallics* **1987**, *6*, 328.

(4) Young, D. C.; Howe, D. V.; Hawthorne, M. F. *J. Am. Chem. Soc.* **1969**, *91*, 859.

(5) Manuscript for the formation of neutral carborane derivatives in preparation.

(6) Spectroscopic data are as follows: IR spectrum (KBr): 2989 (w), 2590 (s), 2549 (vs), 1458 (m), 1397 (m), 1183 (w), 1164 (w), 1091 (w), 1025 (m), 1011 (m), 940 (w), 917 (m), 822 (w), 788 (w), 742 (w) cm^{-1}. ^1H NMR (ppm, CD_2Cl_2, 298 K): 3.1 (qrt, 6 H, $-CH_2-$), 2.0 (s, 2 H, carborane CH), 1.3 (t, 9 H, $-CH_3$). $^{11}B\{^1H\}$ NMR (ppm, THF, 298 K): −12.8, −17.7, −19.8, −22.3, −38.5 (2:3:1:2:1).

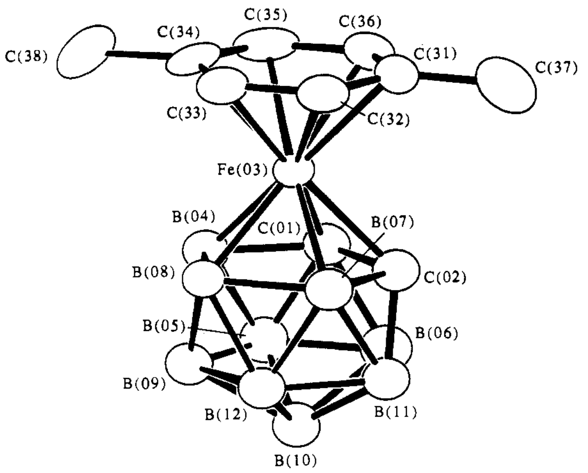

Figure 2. Molecular structure *closo*-3-(η^6-1,4-$(CH_3)_2C_6H_4$)-3,1,2-$FeC_2B_9H_{11}$ (**2**) showing the atom-labeling scheme. All hydrogen atoms have been omitted for clarity.

complexes **1**, **2**, and triethylamine-substituted neutral species were obtained in low yield, the known complex $[Fe^{III}(\eta^5\text{-}C_2B_9H_{11})_2]^-$ (**3**)[2b] was afforded as a major product. The basicity of triethylamine is apparently sufficient to deprotonate the *nido*-7,8-$C_2B_9H_{12}^-$ ion to form a dicarbollide, *nido*-7,8-$C_2B_9H_{11}^{2-}$, that functions as a ligand in these complexes. When less basic nitrogen-containing ligands such as pyridine and acetonitrile were employed in this reaction, ligand-substituted neutral carboranes were exclusively formed in high yields.[8] When ferrous chloride was used instead of ferric chloride in this reaction, only the iron sandwich complex **3** was detected. This result suggests that the formation of **1** and **2** may take place while Fe^{2+} ion is supplied slowly in small amounts from the oxidative substitution reaction as a reduced species. Complexes **1** and **2** are thermally stable neutral orange crystals, although their solutions show color change after exposure to air for 3 days. Their ^{11}B FT NMR spectra are consistent with those of other (η^6-arene)metallacarborane complexes of MC_2B_9,[3a] showing a relative area ratio 1:1:2:2:2:1. In ^1H FT NMR spectra, the peaks assigned to the aromatic ring protons exhibit the upfield shift that has been found for the protons of the complexed arenes.[9]

The structure of **1** was determined by a single-crystal X-ray diffraction study, and the molecule is illustrated in Figure 1. Selected interatomic distances and angles are listed in Table I. Due to the disorder present in the crystal, the bond distances and angles in the toluene ligand in species **1** could not be determined accurately. Thus, we decided to obtain the structure of the closely related complex **2**. The molecular structure of **2** is illustrated in Figure 2, and selected interatomic distances and angles are listed in Table II. As can be seen in the figures, the structures of **1** and **2** exhibit a similar sandwich type geometry with the iron flanked by both the arene ring and the C_2B_3 face of the C_2B_9 cage. C_2B_3 bonding faces in **1** and **2** are planar (maximum deviation of 0.023 and 0.015 Å, respectively) with the iron approximately centered over the ring at distances of 1.494 and 1.480 Å, respectively, from the C_2B_3 plane.[10] The iron atom is also bound in a symmetrical fashion to the arene ring in **1** and **2** with distances of 1.566 and 1.575 Å from the C_6 plane,[11] respectively. The C_6 arene rings in **1** and **2** are also planar (maximum deviation in **2**: 0.016 Å) and almost parallel to the C_2B_3 plane with dihedral angles of 1.8 and 2.2°, respectively.[12] The average of Fe–C (arene) distances of 2.098 (20) Å in **1** and 2.115 (9) Å in **2** are similar to those of other *closo*-FeC_2B_9 arene complexes, e.g. 2.116 (10) Å in *closo*-2-(η^6-$CH_3C_6H_5$)-1,7-$(CH_3)_2$-2,1,7-$FeC_2B_9H_9$[13] and 2.123 (14) Å in *closo*-3-(η^6-$(CH_3)_3C_6H_3$)-3,1,2-$FeC_2B_9H_{11}$,[3a] and slightly longer than the average distance of 2.038 (9) Å in the smaller cage complex 1-(η^6-$CH_3C_6H_5$)Fe-2,3-$(C_2H_5)_2C_2B_4H_4$.[3e]

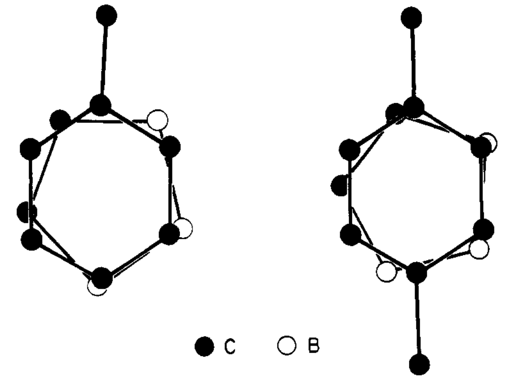

Figure 3. Projections of arene rings onto carborane C_2B_3 planes.

The orientation of the arene rings with respect to the carborane ligand is of interest, and in Figure 3, the arene and the C_2B_3 rings of the carborane ligands in each molecule are projected onto a common plane. Both C_6 rings are staggered with respect to the carbon–carbon edge (C(01)–C(02)). In molecule **1** the C_6 ring is eclipsed with respect to one of the boron–boron edges (B(04)–B(08)); however, in molecule **2** the arene ring shows a nearly eclipsed arrangement to the other boron–boron edge (B(07)–B(08)). The orientation of the methyl groups precludes any possible symmetry in either molecule, although the methyl groups were expected to lie between the carbon–carbon edge of the C_2B_3 face. The fact that the orientation of one of the methyl groups of xylene in **2** and the methyl group of toluene in **1** is similar suggests that they are energetically similar and that they utilize their most favorable conformations. There are no significant intermolecular contacts in either crystal structure.

Experimental Section

All manipulations were carried out under an inert atmosphere with standard Schlenk techniques.[14] All solvents were purified by standard procedures and distilled under nitrogen prior to use. Triethylamine was distilled before use. Infrared spectra were recorded by using KBr pellets on a Beckman Model FT 1100 FT-IR. ^1H NMR spectra were obtained on a Bruker WP-200 FT-NMR spectrometer at 200.133 MHz. ^{11}B NMR spectra were recorded on a Bruker AM-500 FT-NMR spectrometer at 160.463 MHz. Elemental analyses were performed by Galbraith Laboratories, Knoxville, TN.

---

(7) Spectroscopic data are as follows. IR spectrum (KBr): 2984 (w), 2544 (vs), 1474 (m), 1458 (m), 1388 (s), 1184 (w), 1152 (m), 1099 (w), 1049 (w), 1029 (w), 1005 (s), 975 (w), 958 (w), 934 (w), 835 (w), 743 (w) cm^{-1}. ^1H NMR (ppm, CD_2Cl_2, 298 K): 3.2 (qrt, 6 H, $-CH_2-$), 2.3 (s, 1 H, carborane CH), 1.9 (s, 1 H, carborane CH), 1.3 (t, 9 H, $-CH_3$). $^{11}B\{^1H\}$ NMR (ppm, THF, 298 K): 2.8, −6.0, −17.5, −18.1, −19.4, −26.5, −28.5, −32.6, −38.9 (1:1:1:1:1:1:1:1:1).

(8) Young, D. C. Ph.D. Thesis, University of California, Riverside, 1966.

(9) Gastinger, R. G.; Klabunde, K. J. *Transition Met. Chem.* (*N.Y.*) **1971**, *4*, 1.

(10) Fe–C_2B_3 plane distances: (a) 1.48 Å in $[C_6(CH_3)_3H_3]FeC_2B_9H_{11}$.[3a] (b) 1.49 Å in $(C_5H_5)FeC_2B_9H_{11}$ (Zalkin, A.; Templeton, D. H.; Hopkins, T. E. *J. Am. Chem. Soc.* **1965**, *87*, 3988). (c) 1.58 Å in $Cs_2[(C_2B_9H_{11})_2Fe_2(CO)_4]\cdot(CH_3)_2CO\cdot H_2O$ (Greene, P. T.; Briyan, R. F. *Inorg. Chem.* **1970**, *9*, 1464).

(11) Fe–arene plane distances: (a) 1.60 Å in $[C_6(CH_3)_3H_3]FeC_2B_9H_{11}$.[3a] (b) 1.58 (1) Å in $[C_6(CH_3)_6]Fe(C_5H_5)$ (Astruc, D.; Hamon, J.-R.; Althoff, G.; Roman, E.; Batail, P.; Michand, P.; Mariot, J.-P.; Varret, F.; Cozak, D. *J. Am. Chem. Soc.* **1979**, *101*, 5445). (c) 1.59 Å in $[Fe\{\eta\text{-}C_5H_4\text{-}(CH_2)_3\text{-}\eta\text{-}C_6H_5\}][PF_6]$ (Nesmeyanov, A. N.; Tolstaya, M. V.; Rybinskaya, M. I.; Shul'pin, G. B.; Bokii, N. G.; Batsanov, A. S.; Struchkov, Yu. T. *J. Organomet. Chem.* **1977**, *142*, 89). (d) 1.548 Å in $(C_6H_6)Fe[(C_2H_5)_2C_2B_4H_4]$, 1.539 Å in $[C_6(CH_3)_3H_3]Fe[(C_2H_5)_2C_2B_4H_4]$, and 1.554 Å in $[C_6(CH_3)_6]Fe[(C_2H_5)_2C_2B_4H_4]$.[3d]

(12) C_6 plane–C_2B_3 plane dihedral angles: (a) 2.5° in $(CH_3C_6H_5)Fe[C_2B_9H_9(CH_3)_2]$.[3b] (b) 2.9° in $[C_6(CH_3)_3H_3]FeC_2B_9H_{11}$.[3a] (c) 3.30° in $(C_5H_5)FeC_2B_9H_{10}(OCOCF_3\text{-}8)$ (Zakharkin, L. I.; Kobak, V. V.; Kovredov, A. I.; Furmanova, N. G.; Struchkov, Y. T. *Izv. Akad. Nauk SSSR, Ser, Khim.* **1979**, 1097). (d) 2.08° in $(C_6H_6)Fe[(C_2H_5)_2C_2B_4H_4$ and 2.83° in $[C_6(CH_3)_3H_3]Fe[(C_2H_5)_2C_2B_4H_4]$.[3d] (e) 1.2° in $(CH_3C_6H_5)Fe[(C_2H_5)_2C_2B_4H_4]$.[3e]

(13) Garcia, M. P.; Green, M.; Stone, F. G. A.; Somerville, R. G.; Welch, A. J.; Briant, C. E.; Cox, D. N.; Mingos, D. M. P. *J. Chem. Soc., Dalton Trans.* **1985**, 2343.

(14) Shriver, D. F. *The Manipulation of Air-Sensitive Compounds*; McGraw-Hill: New York, 1969.

Table III. Details of Crystallographic Data Collection

	1	2
temp/K	298	298
crystal size/mm	0.13 × 0.26 × 0.45	0.2 × 0.3 × 0.4
normal to faces	$10\bar{1}$, 103, 010	100, 010, 001
appearance	parallelpiped	parallelepiped
radiation (graphite monochromator)	Mo Kα	Mo Kα
wavelength/Å	0.7107	0.7107
space group	$P2_1/c$	$Pna2_1$
a/Å	7.7452 (7)	12.862 (3)
b/Å	8.8974 (9)	7.491 (2)
c/Å	19.6596 (20)	15.002 (3)
β/deg	90.195 (3)	
V/Å^3	1355	1445
Z	4	4
ρ(calcd)/g cm^{-3}	1.37	1.35
μ/cm^{-1}	10.8	10.2
scan width, deg		
below Kα_1	1.3	1.3
above Kα_2	1.6	1.6
scan rate/deg min^{-1}	3.0	3.0
no. of unique reflcns	2386	978
no. of obsd ($I > 3\ \sigma(I)$) reflcns	1588	848
2θ max/deg	50	45
data collcd	$+h,+k,\pm l$	$+h,+k,+l$
no. of params refined	148	125
R	0.08	0.045
R_w	0.11	0.056
GOF	3.49	1.81

Preparation of *closo*-3-(η^6-$CH_3C_6H_5$)-3,1,2-$FeC_2B_9H_{11}$ (1). A 1-L three-neck flask was fitted with a reflux condenser having a gas outlet, a pressure-equalized addition funnel and a gas inlet that was connected to a nitrogen manifold. To the flask were added 1.07 g (6.2 mmol) of K[*nido*-7,8-$C_2B_9H_{12}$], 50 mL of toluene, 11 mL of triethylamine, and a magnetic stir bar. The solution was heated to reflux, and a solution of 2.10 g (13 mmol) of anhydrous ferric chloride in 400 mL of toluene was added dropwise over a period of 1 h to the refluxing solution. The color of the solution slowly changed to dark red. After approximately 15 h of reflux, the reaction mixture was cooled and filtered and the precipitate washed with 100 mL of hot benzene. The combined red filtrates were washed with 200-mL portions of distilled water three times. The washed toluene solution was dried over anhydrous magnesium sulfate, evaporated in vacuo to a volume of 20 mL, and then let stand for a period of 1 week. Brown rod-shaped crystals were formed (0.035 g, 3% yield). ^{1}H NMR (ppm, reference residual solvent protons = 5.32, CD_2Cl_2, 298 K): 6.2 (m, 3 H, aromatic protons), 6.0 (m, 2 H, aromatic protons), 3.8 (s, 2 H, carborane CH), 2.5 (s, 3 H, CH_3). ^{11}B NMR (ppm, reference $BF_3 \cdot OEt_2$, THF, 298 K): 0.1, −3.1, −9.9, −11.1, −21.2, −26.3 (1:1:2:2:2:1).

Preparation of *closo*-3-(η^6-1,4-$(CH_3)_2C_6H_4$)-3,1,2-$FeC_2B_9H_{11}$ (2). The trimethylammonium salt of [*nido*-7,8-$C_2B_9H_{12}$]$^-$ (3.10 g, 15 mmol), anhydrous ferric chloride (2.43 g, 15 mmol), and 20 mL of triethylamine were treated with *p*-xylene in a manner similar to that described above. Orange crystals were obtained (0.15 g, 5.1% yield). Anal. Calcd for $C_{10}H_{21}B_9Fe$: C, 40.79; H, 7.19; B, 33.05; Fe, 18.97. Found: C, 40.58; H, 6.91; B, 31.71; Fe, 18.42. IR: 3039 (w), 2613 (m), 2530 (vs, br), 1489 (m), 1452 (w), 1375 (m), 1106 (w), 1016 (s), 987 (s), 865 (w) cm^{-1}. ^{1}H NMR (ppm, CD_2Cl_2, 298 K): 5.9 (s, 4 H, aromatic protons), 3.6 (s, 2 H, carborane CH), 2.4 (s, 6 H, CH_3). ^{11}B NMR (ppm, reference $BF_3 \cdot OEt_2$, THF, 298 K): 0.8, −3.0, −9.4, −10.2, −20.6, −25.6 (1:1:2:2:2:1).

Collection and Reduction of X-ray Data for 1. An air-stable crystal, obtained from a toluene solution, was mounted on a thin glass fiber on a diffractometer constructed by Professor C. E. Strouse of this department. Systematic absences were found for reflections $0k0$, $k = 2n + 1$, and for $h0l$, $l = 2n + 1$. Unit cell parameters were determined from a least-squares fit of 43 accurately centered reflections (9.5° < 2θ < 20.5°). These dimensions and other parameters, including conditions of data collection, are summarized in Table III. Data were collected in the θ–2θ scan mode. Three intense reflections (206), (2,0,−6), and (2,3,−1) were monitored every 97 reflections to check stability. Intensities of these reflections fluctuated only slightly, ca. ±4%, during the course of the experiment. Of the 2386 unique reflections measured, 1588 were considered observed ($I > 3\sigma(I)$) and were used in the subsequent structure analysis. Data were corrected for Lorentz and polarization effects but not for absorption effects. Programs used in this work include locally modified versions of the programs listed in the reference section.[15]

Table IV. Positional and Equivalent Isotropic Thermal Parameters for **1**[a]

atom	x	y	z	u^2,[b] Å^2
Fe(03)	0.2495 (3)	0.1931 (1)	0.9035 (1)	0.065
B(08)	0.2490 (17)	−0.0465 (16)	0.9127 (7)	0.066
C(02)	0.3523 (16)	0.1465 (15)	0.8099 (6)	0.073
B(04)	0.0682 (19)	0.0345 (18)	0.8722 (7)	0.074
B(07)	0.4284 (18)	0.0350 (17)	0.8729 (7)	0.070
C(01)	0.1453 (17)	0.1447 (16)	0.8104 (7)	0.074
B(10)	0.2486 (23)	−0.1374 (22)	0.7711 (9)	0.084
B(12)	0.3657 (22)	−0.1535 (20)	0.8497 (9)	0.081
B(09)	0.1399 (21)	−0.1533 (19)	0.8490 (8)	0.078
B(11)	0.4257 (21)	−0.0213 (20)	0.7847 (8)	0.081
B(05)	0.0639 (21)	−0.0240 (20)	0.7855 (8)	0.085
B(06)	0.2462 (23)	0.0511 (21)	0.7455 (9)	0.088
C(36)	0.268 (3)	0.429 (1)	0.9033 (5)	0.035 (4)*
C(35)	0.103 (3)	0.388 (1)	0.9247 (5)	0.063 (6)*
C(34)	0.083 (3)	0.284 (1)	0.9773 (5)	0.069 (6)*
C(33)	0.229 (3)	0.222 (1)	1.0086 (5)	0.050 (5)*
C(32)	0.393 (3)	0.263 (1)	0.9872 (5)	0.053 (5)*
C(31)	0.413 (3)	0.367 (1)	0.9346 (5)	0.055 (5)*
C(21)	0.182 (5)	0.424 (2)	0.904 (1)	0.03 (1)*
C(22)	0.360 (5)	0.406 (2)	0.911 (1)	0.06 (1)*
C(23)	0.427 (5)	0.309 (2)	0.961 (1)	0.14 (2)*
C(24)	0.315 (5)	0.229 (2)	1.003 (1)	0.03 (1)*
C(25)	0.137 (5)	0.246 (2)	0.996 (1)	0.05 (1)*
C(26)	0.070 (5)	0.344 (2)	0.946 (1)	0.07 (1)*
C(37)	0.604 (3)	0.390 (3)	0.916 (1)	0.10 (1)*
C(37′)	−0.107 (4)	0.386 (4)	0.918 (2)	0.07 (1)*

[a] Carbons from C(31) to C(37) are of the arene in the position of major occupancy. Carbons from C(21) to C(26) and C(37′) belong to the disordered arene in the position of lower occupancy. Units of each esd, in parrentheses, are those of the least significant digit of the corresponding parameters. [b] Values marked with an asterisk denote atoms refined with an isotropic thermal parameter. Other isotropic values are $^1/_8\pi^2$ times the "equivalent B value" for an anisotropic atom, as defined by Hamilton: Hamilton, W. C. *Acta Crystallogr.* **1959**, *12*, 609–610.

Solution and Refinement of the Structure of 1. Atoms were located by use of the heavy-atom method. Although they are not quite identical, reflections hkl and $h,k,-l$ are similar in magnitude. Fe lies approximately in a "mirror" plane that bisects the C_2B_9 icosahedron giving positional overlap with large thermal ellipsoids. The arene is disordered about this plane. All calculations were performed on the VAX 11/750 crystallographic computer. All carborane hydrogen atoms were kept in located positions and all arene hydrogen atoms were included in calculated positions, C–H = 1.0 Å, with assigned u values of 0.04 and 0.11 Å^2 for cage and ring H and for methyl H, respectively. Anisotropic thermal parameters were refined for Fe and for cage non-hydrogen atoms. The arene was refined in two positions with occupancies x and $1 - x$, which refined to about 60/40. Each arene ring was constrained to be a rigid hexagon, C–C = 1.395 Å, and each methyl group was constrained to be tetrahedral, H–C–H = 109.5°. Scattering factors for H were obtained from Stewart et al.[16] and for other atoms were taken from ref 17. Anomalous dispersion terms were applied to the scattering of Fe. A final difference electron density map was essentially featureless, the maximum and minimum peaks being about 0.7 e/Å^3. Final positional and thermal parameters for non-hydrogen atoms are given in Table IV.

Collection and Reduction of X-ray Data for 2. An air-stable crystal, obtained from THF/heptane solution, was mounted on a thin glass fiber on a diffractometer constructed by Professor C. E. Strouse of this department. Systematic absences were found for reflections $0kl$, $k + l = 2n + 1$, and for $h0l$, $h = 2n + 1$. Unit cell parameters were determined from a least-squares fit of 22 accurately centered reflections (9.5° < 2θ < 18°). These dimensions and other parameters, including conditions of data collection, are summarized in Table III. Data were collected in the θ–2θ scan mode. Three intense reflections (113), (3,−1,2), and (3,1,−2) were monitored every 97 reflections to check stability. Intensities of these reflections fluctuated only slightly, ca. ±3%, during the course

---

(15) CARESS (Broach, Coppens, Becker, and Blessing), peak profile analysis and Lorentz and polarization corrections; ORFLS (Busing, Martin, and Levy), structure factor calculation and full-matrix least-squares refinement; ORTEP (Johnson), figure plotting; and SHELX76 (Sheldrick), structure analysis package.

(16) Stewart, R. F.; Davidson, E. R.; Simpson, W. T. *J. Chem. Phys.* **1965**, *42*, 3175.

(17) *International Tables for X-ray Crystallography*; Kynoch: Birmingham, England, 1974; Vol. IV.

Table V. Positional and Equivalent Isotropic Thermal Parameters for **2**

atom	x	y	z	10^4U,[a] Å^2
Fe(03)	0.1710 (1)	0.0889 (1)	0.0000	320 (6)
C(01)	0.2203 (8)	0.2532 (14)	–0.0999 (6)	437 (25)*
C(02)	0.2011 (8)	0.0476 (14)	–0.1322 (7)	433 (25)*
B(04)	0.1125 (8)	0.3350 (14)	–0.0478 (8)	389 (25)*
B(05)	0.1416 (9)	0.3923 (15)	–0.1614 (8)	448 (29)*
B(06)	0.2014 (9)	0.2105 (16)	–0.2129 (9)	477 (29)*
B(07)	0.0817 (10)	–0.0299 (18)	–0.1014 (8)	454 (34)*
B(08)	0.0216 (8)	0.1572 (13)	–0.0470 (8)	387 (24)*
B(09)	0.0166 (8)	0.3303 (15)	–0.1307 (7)	424 (26)*
B(10)	0.0688 (8)	0.2571 (16)	–0.2317 (8)	454 (28)*
B(11)	0.1101 (8)	0.0315 (15)	–0.2140 (8)	431 (28)*
B(12)	–0.0049 (8)	0.1048 (14)	–0.1624 (7)	403 (25)*
C(31)	0.2669 (7)	–0.1205 (13)	0.0497 (6)	430 (57)
C(32)	0.1634 (7)	–0.1441 (13)	0.0770 (6)	431 (55)
C(33)	0.1097 (8)	–0.0040 (15)	0.1207 (6)	445 (63)
C(34)	0.1613 (8)	0.1618 (15)	0.1371 (6)	457 (59)
C(35)	0.2617 (8)	0.1855 (14)	0.1071 (7)	491 (64)
C(36)	0.3169 (7)	0.0457 (14)	0.0631 (6)	451 (60)
C(37)	0.3237 (7)	–0.2698 (14)	0.0009 (13)	671 (59)
C(38)	0.1024 (10)	0.3104 (16)	0.1834 (8)	741 (86)

[a] $U_{eq} = {}^1/_6\pi^2\sum\sum\beta_{ij}a_ia_j$. Values marked with an asterisk denote atoms refined with isotropic thermal parameter.

of the experiment. Of the 978 unique reflections measured, 848 were considered observed ($I > 3\sigma(I)$) and were used in the subsequent structure analysis. Data were corrected for Lorentz and polarization effects but not for absorption effects.[15]

Solution and Refinement of the Structure of 2. Atoms were located by use of the heavy-atom method. All calculations were performed on the VAX 11/750 crystallographic computer. All carborane hydrogen atoms were kept in located positions and all xylyl hydrogen atoms were included in calculated positions, C–H = 1.0 Å, with assigned B values of 4.0 and 7.0 Å^2 for cage and ring H and for methyl H, respectively. Anisotropic thermal parameters were refined for Fe and for arene non-hydrogen atoms. Scattering factors for H were obtained from Stewart et al.[16] and for other atoms were taken from ref 17. Anomalous dispersion terms were applied to the scattering of Fe. A final difference electron density map was essentially featureless, the maximum and minimum peaks being about 0.6 e/Å^3. Final positional and thermal parameters for non-hydrogen atoms are given in Table V.

Acknowledgment. We gratefully acknowledge financial support provided by the Office of Naval Research. We also thank Dr. A. Varadarajan for informative discussions.

Registry No. **1**, 110045-26-6; **2**, 110045-27-7; **3**, 65465-56-7; K-[*nido*-7,8-$C_2B_9H_{12}$], 12304-72-2; $FeCl_3$, 7705-08-0; Me_3NH[*nido*-7,8-$C_2B_9H_{12}$], 12543-22-5.

Supplementary Material Available: Tables of positional and thermal parameters of hydrogen atoms, anisotropic thermal parameters, and interatomic distances and angles (14 pages); listings of observed and calculated structure factors (12 pages). Ordering information is given on any current masthead page.

Contribution from the Department of Molecular
Spectroscopy, Research Institute of Materials,
University of Nijmegen, Toernooiveld,
6525 ED Nijmegen, The Netherlands

Spin–Orbit Contribution to the Zero-Field-Splitting Tensor in Weakly Interacting $S = {}^1/_2$ Dimers

M. C. M. Gribnau and C. P. Keijzers*

Received April 3, 1987

It is the purpose of this note to clarify the role of the spin–orbit coupling in the zero-field-splitting (ZFS) tensor of weakly interacting $S = {}^1/_2$ dimers. Moriya[1,2] was the first to derive an analytical expression for this contribution in infinite crystals. In recent years much experimental work[3,4] has been done in order to establish the magnitude of the spin–orbit contribution (which is also called "pseudodipolar interaction" or "anisotropic exchange") to the ZFS in weakly coupled copper dimers with oxygen-,[5–9] sulfur-,[9,10] fluorine-,[11] chlorine-,[12,13] and nitrogen-based[14–16] bridges. The ZFS consists of two contributions, which cannot be measured independently: the dipole–dipole interaction and the spin–orbit contribution. Therefore, the procedure to obtain the spin–orbit contribution is to subtract the calculated dipole–dipole interaction from the experimental ZFS tensor. In the interpretation of the spin–orbit contribution using the theory of Moriya approximations are necessary which are, however, not always valid. In the course of time, the approximate method of interpretation developed a momentum of its own. We have the impression that authors do not always realize that they are using approximate expressions instead of the original exact one of Moriya. The value of the interpretations may, therefore, be very limited. In the following we will first summarize the theory of Moriya. Subsequently, we will clarify the nature of the approximations on the basis of an alternative derivation.

Moriya[1,2] included spin–orbit coupling into Anderson's theory of superexchange.[17,18] Using a third-order perturbation treatment in which both the spin–orbit and the isotropic exchange act as perturbations, he derived an expression that was reformulated for dimeric systems by Kanamori.[19,20] It contains terms such as

$$\frac{\langle g_1g_2|\vec{L}_1\cdot\vec{S}_1|e_1g_2\rangle\langle e_1g_2|\mathcal{H}_{ex}|e_1g_2\rangle\langle e_1g_2|\vec{L}_1\cdot\vec{S}_1|g_1g_2\rangle}{(E_e - E_g)^2}$$

Here g_1 and g_2 represent the orbital singlet ground states of the monomers with energy E_g and e_1 is an excited state monomer orbital of energy E_e. The approximation mentioned above is that the term in $\mathcal{H}_{ex}$ is replaced by a simple two-electron exchange integral, while, in fact, it represents a singlet–triplet splitting of an excited state. This approximation is analogous to approximating the singlet–triplet splitting of the dimer ground state by a simple exchange integral. However, Anderson[17,18] and, more recently, Kahn and co-workers[21] have shown that the singlet–triplet splitting ($2J_0$ in the effective Heisenberg spin Hamiltonian $-2J_0\vec{S}_1\cdot\vec{S}_2$) in the ground state may, in first order, be calculated according to

$$2J_0 = 4tS + 2(j - kS^2) \qquad (1)$$

where t, S are one-electron integrals and j, k are two-electron integrals. The approximation $2J_0 = 2j$ is correct only if the monomer oribitals are orthogonal. This means that the approx-

---

(1) Moriya, T. In *Magnetism*; Rado, G. T., Suhl, H., Eds.; Academic: New York, 1963; Vol. 1, p 85.
(2) Moriya, T. *Phys. Rev.* **1960**, *120*, 91.
(3) *Magneto-Structural Correlations in Exchange Coupled Systems*; Willett, R. D., Gatteschi, D., Kahn, O., Eds.; Reidel: Dordrecht, Holland, 1985.
(4) Keijzers, C. P. In *Electron Spin Resonance*; Symons, M. C. R., Ed.; Special Periodical Reports; Chemical Society: London, 1987; Vol. 10B.
(5) Bencini, A.; Gatteschi, D.; Zanchini, C. *Inorg. Chem.* **1985**, *24*, 700.
(6) Ozarowski, A.; Reinen, D. *Inorg. Chem.* **1986**, *25*, 1704.
(7) Banci, L.; Bencini, A.; Gatteschi, D. *J. Am. Chem. Soc.* **1983**, *105*, 761.
(8) Kokoszka, G. F.; Allen, H. C.; Gordon, G. *J. Chem. Phys.* **1967**, *46*, 3013.
(9) Van Rens, J. G. M.; Van der Drift, E.; De Boer, E. *Chem. Phys. Lett.* **1972**, *14*, 113.
(10) Van Rens, J. G. M.; De Boer, E. *Mol. Phys.* **1975**, *29*, 1743.
(11) Hefni, M. A.; McConnell, N. M.; Rietmeijer, F. J.; Gribnau, M. C. M.; Keijzers, C. P. *Mol. Phys.* **1986**, *47*, 1283.
(12) Chow, C.; Willett, R. D. *J. Chem. Phys.* **1973**, *59*, 5903.
(13) Bencini, A.; Gatteschi, D.; Zanchini, C. *Inorg. Chem.* **1985**, *24*, 704.
(14) Boillot, M. L.; Journaux, Y.; Bencini, A.; Gatteschi, D.; Kahn, O. *Inorg. Chem.* **1985**, *24*, 263.
(15) Felthouse, T. R.; Hendrickson, D. N. *Inorg. Chem.* **1978**, *17*, 444.
(16) Bencini, A.; Gatteschi, D.; Zancini, C.; Haasnoot, J. G.; Prins, R.; Reedijk, J. *Inorg. Chem.* **1985**, *24*, 2812.
(17) Anderson, P. W. In *Magnetism*; Rado, G. T., Suhl, H., Eds; Academic: New York, 1963; Vol. 1, p 25.
(18) Anderson, P. W. *Phys. Rev.* **1959**, *115*, 2.
(19) Kanamori, J. In *Magnetism*; Rado, G. T., Suhl, H., Eds.; Academic: New York, 1963; Vol. 1, p 127.
(20) Owen, J.; Harris, E. A. In *Electron Spin Resonance*; Geschwind, S., Ed.; Plenum: New York, 1972; p 427.
(21) Girerd, J. J.; Journaux, Y.; Kahn, O. *Chem. Phys. Lett.* **1981**, *82*, 534.

0020-1669/87/1326-3413$01.50/0